9th Asia-Pacific Conference on Wind Engineering
Auckland, New Zealand
3-7 December 2017

CFD Simulation of Unbalanced Snow Accumulation due to Wind on a Two-level Flat-roof Model

Y. Murayama, K. Igarashi, and Y. Tominaga

Department of Architecture and Building Engineering
Niigata Institute of Technology, Fujihashi 1719, Kashiwazaki, Japan

Abstract

In this study, unbalanced snow accumulation on a two-level flat-roof building was modeled based on computational fluid dynamics (CFD) using a snowdrift model previously proposed by the authors. Comparison of the predicted snow accumulations with observational data indicate that the observational data of snow depth on the lower roofs could generally be reproduced using the proposed CFD simulation method. However, the specific undulations of snow are not well reproduced by CFD.

Introduction

When predicting snow loads on building roofs, unbalanced snow accumulation due to wind flow is a difficult problem. Accumulation occurs because of a complex interaction between snow particle motion and fluid flow, which is affected by building geometry. Through field observations, much has been learned about this phenomenon [7, 10, 12, 17]. Observation of specific cases in which the impacts of various parameters on snow accumulations were considered under controllable conditions (e.g., wind or water tunnels) has also been effective in advancing knowledge [3, 5, 8, 18]. Although these efforts have contributed significantly to improvements in building design [4], their applicability has been limited to specific geometries and weather conditions. Recently, computational fluid dynamics (CFD) was applied to prediction of snowdrift around buildings [14]. However, few studies have applied CFD to prediction of roof snow. Thiis et al. [11] predicted snow distribution on a sports hall with a curved roof located in Oslo, Norway, and compared the simulated results with field measurements. They focused primarily on reproducing the snow distributions observed on the actual building caused by the specific weather conditions. Only a few prior studies have applied CFD to model snowdrifts with a generic configuration (e.g., [19]).

Tominaga et al. [15] conducted CFD simulations of unbalanced snow accumulation on roofs for an isolated gable-roof building. In their study, they confirmed that the proposed CFD simulation method generates results that are congruent with actual observational results. Consistent with observational results, the model showed that the snow depth on the leeward side of the roof increases with increasing wind velocity and roof pitch. However, applicability of the proposed CFD method needs to be examined for other configurations. In this study, the proposed snowdrift model is applied to prediction of snow distribution on a two-level flat-roof building, and snow depth distributions measured in Hokkaido, Japan [12, 17] were compared with the simulated results.

CFD Simulation Method

Building configuration

Figure 1 presents a schematic view of the building model used in this study. This model was adopted from the detailed field measurement in Hokkaido, Japan conducted by Tsuchiya et al. [12, 17]. An isolated stepped flat-roof building, with roof height 1.8 m (2H), width 5.4 m (6H), and length 4.5 m (5H), was placed perpendicular to the approaching wind flow. In this study, the following two cases were considered: (1) lower roof located on the leeward side (leeward case) and (2) lower roof located on the windward side (windward case).

In the field measurements, the snow distributions were measured after one snowdrift event. That is, after the measurement, all the snow on and around the building was removed in preparation for the next measurement. In this study, three snowdrift events, in which the wind directions were virtually perpendicular to the building, were considered for each case. The mean wind velocity, U_{mean}, and the increased depth of ground snow, S_d, during each snowdrift event are indicated in Table 1.

Table 1. Conditions for each snowdrift event.

Conditions	U_{mean}	S_d
A	2.9 m/s	7 cm
B	2.3 m/s	30 cm
C	1.2 m/s	11 cm

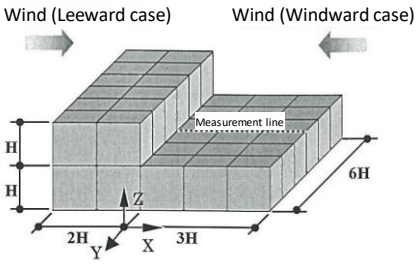

Figure 1. Building model [12, 17]

Numerical methods

The ANSYS FLUENT 14.5 commercial software was used to perform steady-state Reynolds-averaged Navier-Stokes (RANS) equation computations based on a control volume approach to solve the flow equations [1]. The realizable k-ε model [9] was used as the turbulence model.

The computational conditions used in this study are based on guidelines from the Architectural Institute of Japan (AIJ) [13]. At the inlet, a power law profile with an index of 0.20 was assumed for mean streamwise velocity U; the profile for k was determined using a turbulent intensity equation proposed by the AIJ [2]. The standard wall functions were applied to the wall boundaries. Symmetric boundary conditions were imposed at the sides and top of the domain, implying zero normal velocity and zero gradients for all the variables at these boundaries. Zero static pressure was imposed at the outlet of the domain.

The computational domain encompassed a volume of 50 m (x) × 40 m (y) × 30 m (z), which was discretized into approximately 1.0 million hexahedral cells, as shown in Figure 2. The building

width and height were divided into approximately 20 and 60 cells, respectively. A grid sensitivity analysis showed that grid refinement did not significantly affect the results.

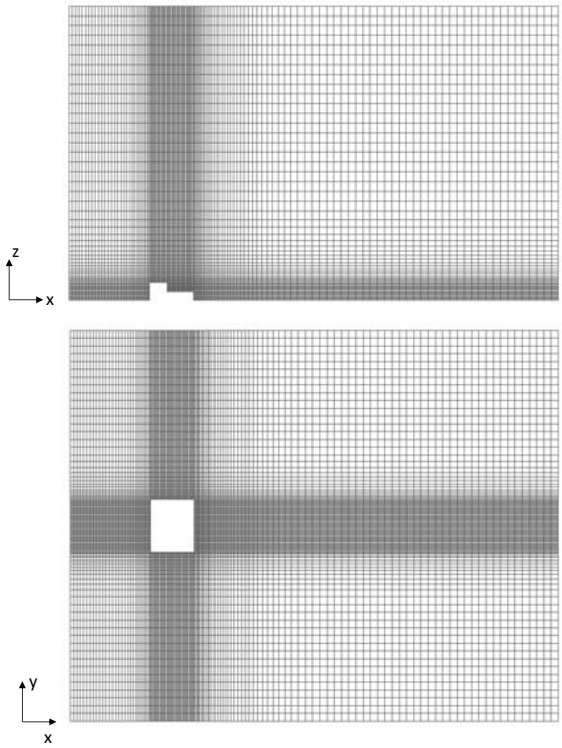

Figure 2. Computational domain and grid discretization

Drifting snow field

The method used to calculate the snow depth ratio is outlined in Figure 3. The snowdrift model previously proposed by the authors [14] was implemented in CFD code as a user-defined function. To model suspension, the transport equation for snowdrift density (Φ) [kg/m^3] was solved, where W_f is the snowfall settling velocity, assumed to be -0.5 m/s:

$$\frac{\partial \Phi}{\partial t} + \frac{\partial U_i \Phi}{\partial x_i} + \frac{\partial W_f \Phi}{\partial x_3} = \frac{\partial}{\partial x_i}\left(\frac{\nu_t}{\sigma_s}\frac{\partial \Phi}{\partial x_i}\right) \quad (1)$$

The snowdrift density at the inflow and top boundaries (Φ_{in}) was 7.5×10^{-4} kg/m^3, calculated using the amount of snowfall per unit time and snowfall velocity (W_f). The turbulent Schmidt number (σ_s) was 0.7 [16].

The deposition flux on the snow surface (q_{dep}) [kg/m^{2}s] and the erosion flux on the snow surface (q_{ero}) [kg/m^{2}s] were determined using Eqs. (2) and (3) as follows:

$$q_{dep} = W_f \Phi_P \left(\frac{U_{*t}^2 - U_*^2}{U_{*t}^2}\right) \quad (U_* \le U_{*t}) \quad (2)$$

$$q_{ero} = -A_e \rho_i U_* \left(1 - \frac{U_{*t}^2}{U_*^2}\right) \quad (U_* > U_{*t}) \quad (3)$$

where Φ_P is the drift density at the first grid adjacent to the snow surface, U^* is the friction velocity at the snow surface, U^*_t is the threshold friction velocity (0.2 m/s), Ae is a proportional constant (1.0×10^{-5}), and ρ_i is the density of ice. This model differs from the prior study's model [14] because friction velocity effects on the snow surface were included in not only erosion but also deposition fluxes [6]. The net deposition flux (q_{total}) [kg/m^{2}s] is given by Eq. (4):

$$q_{total} = q_{dep} + q_{ero} \quad (4)$$

When erosion occurs ($U^* > U^*_t$), q_{ero} is given as the surface boundary condition for the Φ transport equation.

Friction velocity (U^*) was calculated using a generalized log law adopted in CFD code [1] as follows:

$$U_*^2 = \frac{\kappa C_\mu^{1/4} k_P^{1/2} U_P}{ln\left(\frac{E C_\mu^{1/4} k_P^{1/2} y_P}{\nu}\right)} \quad (5)$$

where

U_P is the mean velocity of the fluid at point P
k_P is the turbulent kinetic energy at point P
y_P is the distance from point P to the wall
ν is the kinematic viscosity of the fluid
E = 9.793, κ = 0.4187, C_μ = 0.09

In this study, snow depth was not calculated directly. The snow depth ratio was defined as the ratio between the standard deposition flux ($q_{sta} = \Phi_{in} \times W_f$) and net deposition flux (q_{total}). The snow depth ratio was calculated using the net deposition flux at the reference point, which was not affected by the building.

The snowdrift analysis was performed using steady-state CFD, in which the flowfield is unaffected by snow accumulation. Thus, the results of this analysis express the potential for snow deposition or erosion due to the flowfield determined by the building geometry without snow. Although, surface change effects can be considered using sequential predicted snow surface levels and grid deformation [11, 19], such an approach is time-consuming and complicated. In this study, the applicability of the one-way method that does not consider the influence of surface change on the flowfield, was examined from a practical viewpoint.

In steady-state CFD simulation, a mean wind velocity is applied as a boundary condition. In the real environment, wind velocity fluctuates over time during snowdrift formation; erosion and deposition do not occur continually. This real phenomenon is difficult to reproduce accurately using steady-state CFD. In this study, a simplified method to reproduce this process was proposed for steady-state CFD. Specifically, the weighted average of prediction results for different wind velocities was used to obtain the snowdrift result at a specific reference velocity. In this study, the occurrence frequency of the wind velocities was assumed to follow a normal distribution. Accordingly, the occurrence probabilities of U_{ave}, U_{ave} ± 1 m/s, and U_{ave} ± 2 m/s were assumed to be 40%, 25%, and 5%, respectively, to obtain the averaged snowdrift result for U_{ave} at the building height.

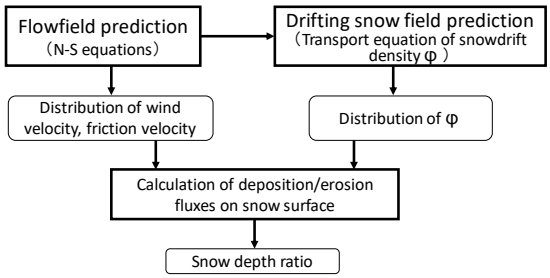

Figure 3. Outline of snowdrift calculation.

Results and Discussion

Velocity field

Figure 4 compares the velocity vectors obtained by the wind tunnel experiment for the same configurations [12, 17] and the

streamlines obtained by the present CFD for each case. It confirms that the flow pattern is independent of the incoming velocity. For the windward case, a small standing vortex is observed on the lower roof. The general patterns of the flowfield are very similar between the experiment and CFD. For the leeward case, there is a large recirculation flow on the lower roof. It should be noted that the wind directions on the lower roofs are opposite to the approaching wind direction for both cases.

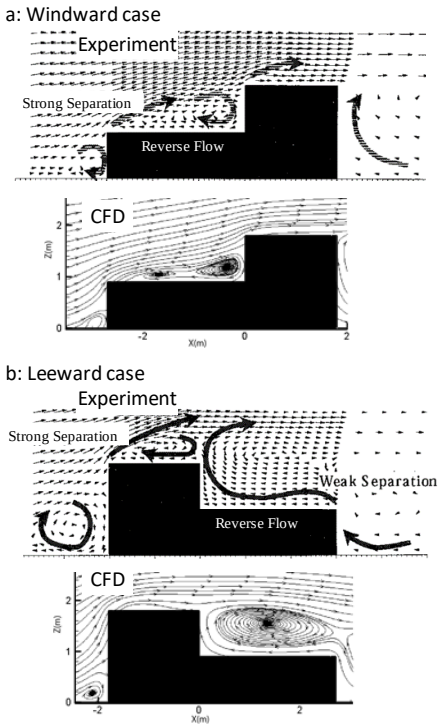

Figure 4. Comparisons of velocity vectors obtained by wind tunnel experiment [12, 17] and streamlines by CFD: (a) Windward case, (b) Leeward case.

Roof snow accumulation

Figure 5 shows the resulting snow depth ratio distributions on the roof and ground surfaces obtained by CFD with the different approaching wind velocities for the windward case. With U = 2.0 m/s, there is virtually no change in the snow depth ratio on the lower roof. With U = 3.0 m/s and over, snow is gradually eroded mainly near the edge of the lower roof. Figure 6 compares the resulting snow depth ratio distributions on the roof and ground surfaces obtained by CFD for the leeward case. With U = 2.0 m/s, there is also no change in the snow depth ratio on the lower roof. With U = 3.0 m/s and over, snow is more eroded on the lower roof than in the windward case, except for just behind the higher roof.

Figure 7 compares the snow depth ratios obtained by CFD and the field measurement at the centerlines for both cases. The measurement data were collected under the three different weather conditions shown in Table 1. U_{ave} indicates the mean wind velocity used for the weighted average mentioned earlier. For the windward case, the snow distributions on the middle of the lower roof are virtually flat in the measurements, and are almost independent of the wind velocity. This tendency is reproduced well in the CFD results. Furthermore, near the windward edge, CFD reproduced the tendency of the snow depths to decrease according to the increase in the wind velocity. However, a large undulation near the higher roof, observed in the measurement with the large velocity condition (cond. A), is not reproduced in CFD. For the leeward case, CFD also reproduced the tendency of the snow depths to decrease according to the increase in the wind velocity. However, a large undulation behind the higher roof is also not reproduced in CFD for this case.

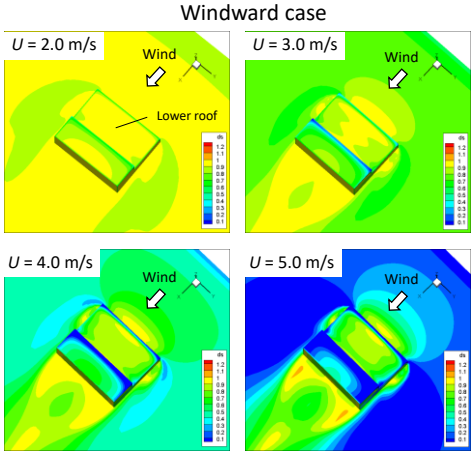

Figure 5. Distributions of snow depth ratio on the roof and ground surfaces obtained by CFD for the windward case

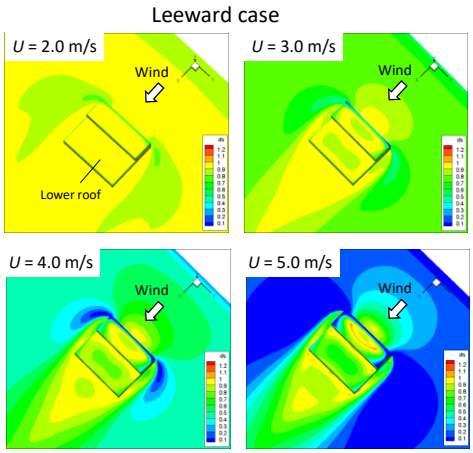

Figure 6. Distributions of snow depth ratio on the roof and ground surfaces obtained by CFD for the leeward case

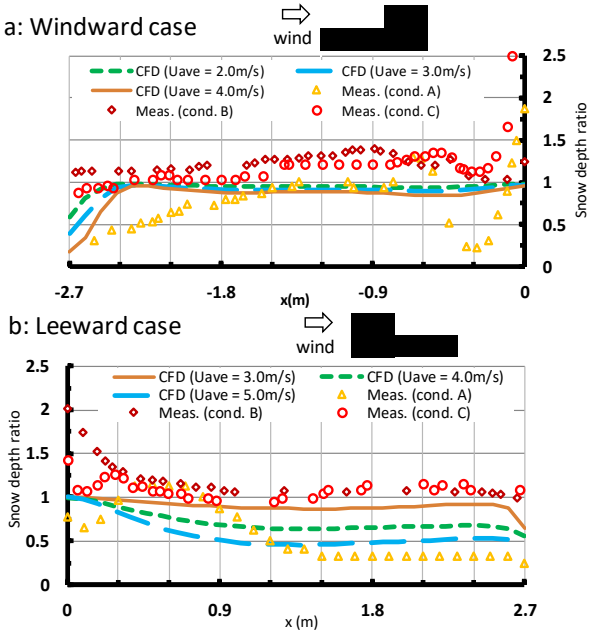

Figure 7. Comparison of snow depth ratios between CFD and field measurement: (a) Windward case, (b) Leeward case.

Conclusions

In this study, CFD simulations of unbalanced snow accumulation on roofs were conducted for an isolated two-level flat-roof building and the results compared with observational data.

The followings are the contributions of this work:

- A prediction method, in which results obtained for different wind velocities are combined assuming a normally distributed occurrence frequency for wind velocities, was proposed.
- The proposed CFD simulation method is generally able to reproduce observational results, in which the snow depths decrease according to the wind velocity.
- However, the large undulations near the higher roof observed in the measurement are not well reproduced in CFD. This may be attributable to the fact that the temporal change in snow surface was not considered in the present computation.

The current study has the following limitations that will be addressed in future work:

- The validity of the model parameters, such as threshold friction velocity and snowfall settling velocity, were not examined and optimized for various conditions.
- This study only considered wind direction perpendicular to the windward facade. The effect of wind direction variations need to be considered.

Acknowledgments

The authors would like to express gratitude for financial support provided through Grants-in-Aid for Scientific Research in Japan (No. 16H04467).

References

[1] ANSYS Fluent, *ANSYS Fluent Theory Guide, Release 14.5*, ANSYS Inc., Canonsburg, PA., 2012.

[2] Architectural Institute of Japan, *AIJ Recommendations for Loads on Buildings (2004Edition)*, 2006.

[3] Dufresne de Virel, M., Delpech, P. & Sacre, C., Wind tunnel investigation of snow loads on buildings, in *Snow Engineering*, editors Hjorth-Hansen, Holand, Loset & Norem, 2000, 171-178.

[4] ISO 4355 'Bases for design of structures - Determination of snow loads on roofs', 2013.

[5] Isyumov, N. & Mikitiuk, M., Wind tunnel model tests of snow drifting on a two-level flat roof, *J. Wind Eng. Ind. Aerodyn.*, **36**, 1990, 893-904.

[6] Naaim, M., Naaim-Bouvet, F. & Martinez, H., Numerical Simulation of drifting snow: erosion and deposition model, *Ann. Glaciol.*, **26**, 1998, 191-196.

[7] O'Rourke, M.J., Asce, M., Speck, Jr., R.S., Asce, A.M. & Stiefel, U., Drift snow loads on multilevel roofs, *J. Struct. Eng.*, **111**(2), 1985, 290–306.

[8] O'Rourke, M.J. & Wrenn, P., Water flume evaluation of snowdrift loads on two-level flat roofs, in *Snow Engineering: Recent Advances*, editors Izumi, Nakamura & Sack, 1997, 321-328.

[9] Shih, T.H., Liou, W.W., Shabbir, A., Yang, Z. & Zhu, J., A new k-ε eddy viscosity model for high Reynolds number turbulent flows: Model development and validation, *Comput. Fluids*, **24**(3), 1995, 227-238.

[10] Taylor, D.A., Roof snow loads in Canada, *Canadian J. of Civil Eng.*, **7**(1), 1980, 1-18.

[11] Thiis, T.K., Potac, J. & Ramberg, J.F., 3D numerical simulations and full scale measurements of snow depositions on a curved roof, in *5th European & African Conference on Wind Engineering*, Florence, Italy, 2009.

[12] Tomabechi, T., Hosokawa, K. & Tsuchiya, M., Field measurement of snowdrift on a two-level flat roof model, *Seppyo*, **65**(3), 2003, 231-239. [in Japanese]

[13] Tominaga, Y., Mochida, A., Yoshie, R., Kataoka, H., Nozu, T. Yoshikawa, M. & Shirasawa, T., AIJ guidelines for practical applications of CFD to pedestrian wind environment around buildings, *J. Wind Eng. Ind. Aerodyn.*, **96**(10-11), 2008, 1749-1761.

[14] Tominaga, Y., Okaze, T. & Mochida, A., CFD modeling of snowdrift around a building: An overview of models and evaluation of a new approach, *Build. Environ.*, **46**(4), 2011, 899-910.

[15] Tominaga, Y., Okaze, T. & Mochida, A., CFD simulation of drift snow loads for an isolated gable-roof building, in *8th International Conference on Snow Engineering*, Nantes, France, June 14-17, 2016, 208-214.

[16] Tominaga, Y. & Stathopoulos, T., Turbulent Schmidt numbers for CFD analysis with various types of flowfield, *Atmos. Environ.*, **41**(37), 2007, 8091-8099.

[17] Tsuchiya, M., Tomabechi, T., Hongo, T. & Ueda, H., Wind effects on snowdrift on stepped flat roofs, *J. Wind Eng. Ind. Aerodyn.*, **90**, 2002, 1881-1892.

[18] Zhou, X., Hu, J. & Gu, M., Wind tunnel test of snow loads on a stepped flat roof using different granular materials, *Nat. Hazards.*, **74**, 2014, 1629-1648.

[19] Zhou, X., Kang, L., Gu, M., Qiu, L. & Hu, J., Numerical simulation and wind tunnel test for redistribution of snow on a flat roof, *J. Wind Eng. Ind. Aerodyn.*, **153**, 2016, 92-105.